RANS SOLUTIONS IN COUETTE FLOW WITH STREAMWISE VORTICES

P. R. Spalart
Boeing Commercial Airplanes
PO Box 3707, Seattle 98124, USA
philippe.r.spalart@boeing.com

A. Garbaruk and M. Strelets
New Technologies & Services
St-Petersburg 197198, Russia
strelets@mail.rcom.ru

ABSTRACT

Plane Couette flow is solved for with conventional Reynolds-Averaged Navier-Stokes (RANS) turbulence models, without temporal (t) or streamwise (x) dependence, but with periodic conditions in the lateral z direction and non-zero velocity components in all three directions. Thus, (U,V,W) are functions of (y,z). This is motivated by experimental and DNS observations of large and powerful streamwise vortices with minimal t and x dependence, which raised the possibility that RANS models may allow such vortices to form, with a defendable scale separation away from the modeled turbulence. We find that some RANS models indeed support vortices, which then make a large (near 50%) contribution to the momentum transport in the core region and tangibly increase the skin-friction coefficient C_f at a given Reynolds number, in broad agreement with DNS results and some experiments. The velocity profile with vortices follows the logarithmic law much longer than it does without vortices or in Poiseuille flow, a fact we actually view as largely fortuitous. To date, only models equipped with a Quadratic Constitutive Relation (QCR) have succeeded in creating the vortices. The Linear Eddy-Viscosity Models (LEVM) tested damp the vortices, and return unidirectional solutions with only U varying with y; so did an Explicit Algebraic Reynolds Stress Model. The existence of such "2.5D" solutions is favorable in terms of agreement with experiment and may partly explain the wide experimental scatter, and also a warning of the possible appearance of striations in routine 3D CFD solutions. It is also a warning that the results of Direct Numerical Simulation will depend noticeably on the lateral period, unless it is made very large.

INTRODUCTION

Couette flow is a very simple case, arguably even simpler conceptually than Poiseuille ("channel") flow in that the total shear stress is constant from wall to wall. However, many RANS models which are accurate enough in Poiseuille flow (although calibrated in the boundary layer) under-predict the shear stress in Couette flow, in the center region. This is based on reference data from both experiments and Direct Numerical Simulation (DNS). This is a puzzling fact, but Couette flow has a peculiarity which we are exploring here. This flow even fully turbulent and developed contains large quasi-steady near-streamwise vortices, confirmed both in DNS and some experiments (Lee & Kim 1991; Komminahoi et al. 1996; Kitoh et al. 2005, 2008; Tsukahara et al. 2006).

In DNS, this much longer correlation in the streamwise direction is a serious obstacle, because it leads to very long domains if the two-point correlations are to fall properly to 0; it could also delay statistical convergence, and worsen the dependence on the lateral period of the simulations, which now needs to fit a rather small number of permanent vortices. This is relative to Poiseuille flow again. In experiments, the elongated flow structures could also lengthen the entry region, and exacerbate the sensitivity to any non-uniformity at the inflow as happens for Görtler vortices. Experiments are difficult, in addition, because of the moving wall (Robertson & Johnson 1970; El Telbany & Reynolds 1982). As a result, Couette flow is not known as precisely as Poiseuille flow.

These observations led us to the framework described in the abstract. With the strong presumption that the vortices can effect significant momentum transfer, there is potential to improve the accuracy of RANS predictions, while exploring a somewhat new mode of operation for these models: this momentum transfer is added to the transfer supported by the modeled Reynolds stress. This is similar to Large-Eddy Simulations (LES), in which we distinguish the "resolved" and "modeled" Reynolds stresses after Reynolds-averaging of the solution. However LES has no separation of scales between resolved and modeled turbulent motions, whereas here we do assume a separation of scales; this is needed to justify using the standard RANS form of the model (these are not Detached-Eddy Simulations). The RANS model is operating with mild rates of change in the lateral direction and the time direction (in a Lagrangian sense). In addition, in LES the split between resolved and modeled stress varies with grid resolution, and in a well-conducted LES, strongly favors the resolved stress.

Note that the scale separation between the global vortices and small-scale turbulence is more convincing in this

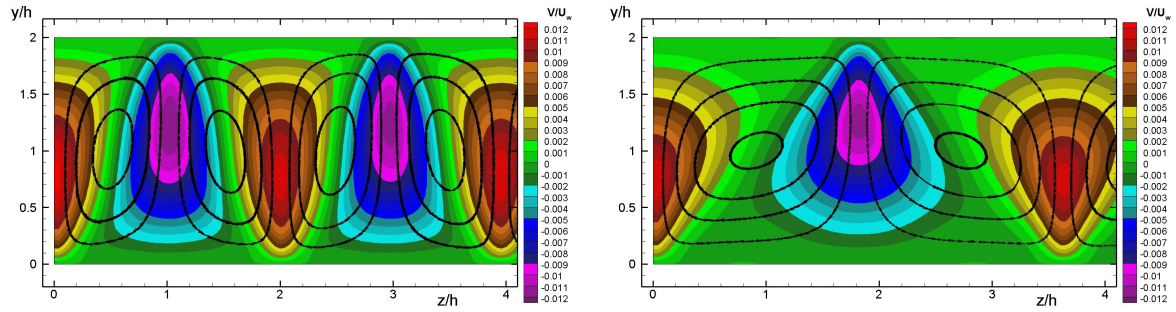

Figure 1. Streamlines of secondary flow, and wall-normal velocity contours. The period Λ_z equals $2h$, left, and $3.64h$, right.

concept than in some that are superficially similar, such as two-dimensional unsteady RANS for vortex shedding past a bluff body. It is still not exact; it could be compared with the use of RANS models in a channel flow with time-varying mass flow. This use is justified when the frequency of the variation is much smaller than the shear rate.

The paper will now briefly present the methods used, followed by primary and then secondary results, and the outlook.

METHOD

Turbulence Models

The baseline model is the one-equation eddy-viscosity model of Spalart & Allmaras (SA, 1994), but the Quadratic Constitutive Relation (QCR) plays an important role here. It was presented under a different name by Spalart (2000). It is a relatively simple nonlinear constitutive relation giving the Reynolds stresses, which overlaps with many contributions in the RANS literature, but is applicable to one-equation models. This constitutive relation introduces the product of the strain tensor S_{ik} and the rotation tensor Ω_{kj} in the Reynolds stress τ_{ij}. Its only adjustable constant was set to $C_{cr1} = 0.3$ to render the Reynolds-stress anisotropy in boundary layers. It was not adjusted to perform in the present application. It was known to correctly generate streamwise vortices in square ducts, and other corner flows, thanks to a more accurate anisotropy, specifically between the wall-normal and the lateral Reynolds stresses ($\overline{w'^2} > \overline{v'^2}$). This suggested that the envisioned Couette-flow vortices may respond strongly to QCR, which they indeed do.

Numerical Aspects

The NTS code (Shur et al. 2004) is used to solve the steady incompressible 2.5D RANS equations with 3rd-order upwind-biased differencing for the inviscid fluxes and 2nd-order centered differencing for the viscous fluxes. The span size of the domain varies from $4h$ up to $40h$. The grid in the z direction is uniform with spacing equal to $0.04h$ which results in 1000 cells for the widest domain. The y grid is non-uniform (clustering near the walls) and has the first y^+ interval less than 0.1. The stretching ratio is about 1.1 and the maximum step is equal to that in the z direction, which gives the total number of cells equal to 177. The iterative convergence is by about 8 orders of magnitude. A few unsteady cases were run to extract growth rates, with implicit second-order (three-layer backward) time integration.

RESULTS

We begin with the principal results, using figures, and later mention more briefly other results which are not covered in detail for lack of space.

Primary Results

Most of the results are for a Reynolds number of 10^5, based on velocity difference U_w and h, the half-height of the channel. Figure 1 shows streamlines and contours of the wall-normal velocity V in the (y,z) plane. The model is SA, with QCR. The spanwise period Λ_z was varied over a wide range, which showed that the vortices exist if $2 < \Lambda_z/h < 3.64$ at least. Two such fields are shown in the figure, with the expected distorted-oval streamlines, and peak values of V/U_w of the order of 0.01. These are small, but will be seen to support significant shear stress, assisted by the larger values of the U deviations, which reach about $0.045U_w$.

Removing the QCR term, with the same model, makes the vortices disappear. Thus, their presence is not a universal feature of RANS models, and appears to be very sensitive to the anisotropy between $\overline{u'^2}$, $\overline{v'^2}$ and $\overline{w'^2}$, which is where the QCR is directly felt.

In terms of impact on the mean flow, the vortices display a moderate sensitivity to the lateral spacing imposed on them by the periodic conditions, even with wide variations of Λ_z. Figure 2 shows the velocity profiles, averaged in the z direction. The presence of the vortices reduces the slope dU/dy of the velocity profile on the centerline by about a factor of 2, which is considerable. The skin-friction coefficient increases by about 13% when vortices are enabled, which is also a large amount, considering that the layers which are completely dominated by wall proximity and have standard logarithmic behavior account for roughly 80% of the velocity difference.

Figure 3 displays the effect of the vortices on the mean flow, using eddy viscosities. The total shear stress itself is of course uniform. We distinguish the Resolved Shear Stress which arises from the z dependence of the flow field, and the Modeled Shear Stress which is the average of the stress carried by the model. Then we calculate an effective eddy viscosity for each of the stresses (i.e., the ratio of stress to shear rate dU/dy), and normalize it with the friction velocity u_τ and h. This is a convenient way of comparing the two contributions against each other and across cases.

Along this paper, following the literature, we use the quantity $R_s \equiv (h/u_\tau)dU/dy$, i.e., the non-dimensional shear rate on the centerline (using friction velocity, following classical scaling). R_s can be viewed as the centerline value of the shear rate normalized with wall distance and friction velocity, i.e., $(y/u_\tau)dU/dy$, and in a logarithmic layer this

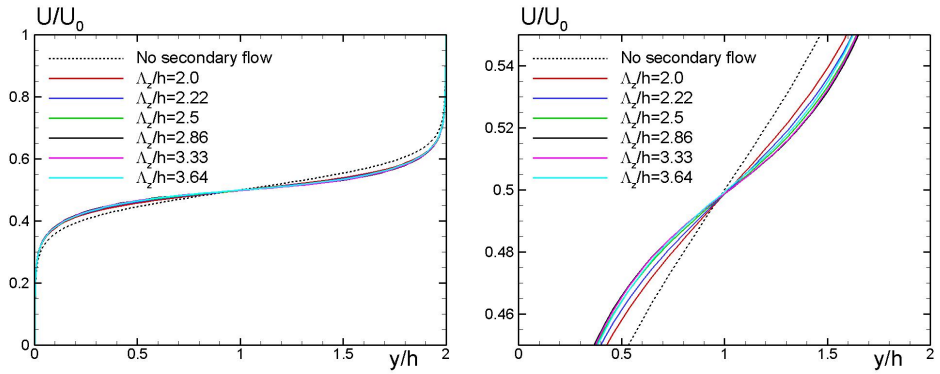

Figure 2. Streamwise velocity profiles without vortices, and with vortices and different values of the lateral period Λ_z. Left, full range; right, detail in center region.

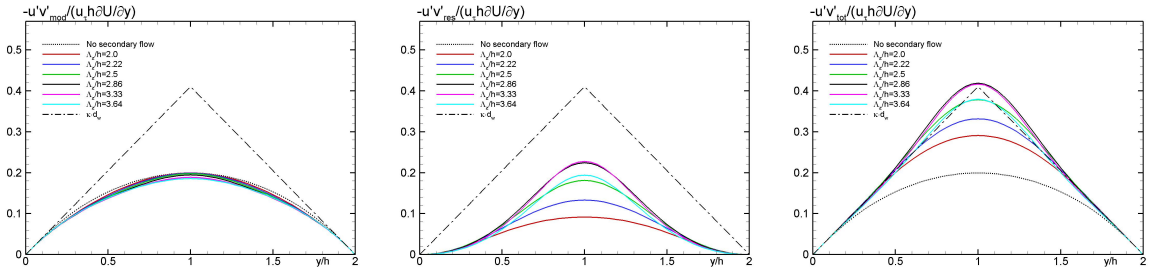

Figure 3. Eddy viscosity attributable to two mechanisms for Reynolds shear stress. Left, modeled stress; center, resolved stress; right, total stress.

quantity takes the value $1/\kappa \approx 2.5$. Its value in laminar flow is $\sqrt{Re/2}$, and would therefore be much larger. R_s is also the inverse of the centerline eddy viscosity, normalized as it is here.

Near the walls, the modeled eddy viscosity equals $\kappa y u_\tau$ as expected, where κ is the Karman constant of the model. The resolved eddy viscosity is proportional to y^3, again as expected with the no-slip condition. In the center region, they are very comparable, with the resolved one slightly larger than the modeled one for the "best" values of Λ_z. The modeled eddy viscosity varies little whether vortices are present or not. Thus, the 2.5D flow is actually radically different from the 2D flow, with the resolved motion (we would not call it resolved turbulence) accounting for about half of the shear stress in the center region. The eddy viscosity in Poiseuille flow would be quite comparable with the modeled viscosity here. This is our key finding: some RANS models accept the large-scale vortices, which in turn dramatically alter the momentum transfer.

This concept is present in Kitoh et al's paper, but their resolved shear stress was much weaker than we are finding. Thus, the quantitative agreement with experiment is fairly poor for the finer quantities of interest. On the other hand, the DNS of Lee & Kim did produce a nearly perfect split, and so the overall agreement in the literature is very loose.

We can loosely examine the separation of scales by comparing the mixing length of the RANS model, which peaks around $0.4h$ (i.e., $l = h/R_s$), and the typical period $\Lambda_z \approx 3h$. They differ appreciably, nearly by an order of magnitude, which is reassuring. The separation expressed this way improves near the walls, of course.

The eddy viscosity with vortices follows the log-law behavior, $\nu_t = u_\tau \kappa y$, much more closely towards the centerline, suggesting to us the most informal description "dome + bell = tent." As a result, the shear rate dU/dy and velocity U also follow log behavior, as confirmed in Figure 4a, strongly confirming a point made by Kitoh et al. that the Couette log region is 2–3 times as wide as the Poiseuille log region. A consequence is that R_s is very close to $1/\kappa$. It is tempting to attribute this wider extent of the log law to the fact that the shear stress is constant in Couette flow, but that is misleading, because the extra shear stress is contributed by motions which span the entire channel, and not by motions which scale with y as required by the theory of wall-bounded turbulence. This point applies equally well to the present framework, which is merely a plausible approximation with some dependence on the RANS model and on the arbitrary choice of Λ_z, and to results of any accuracy from experiments or DNS.

Figure 4b closes in on the end of the velocity profiles, and reveals a significant effect of Λ_z, with a total scatter of about 0.4 U^+ units. In these axes, it is confined to the very end of the curves. It is also much smaller than the effect of suppressing the vortices.

This issue appears especially thought-provoking for DNS, which is normally viewed as directed at near-perfection. Much work has been devoted to the streamwise period Λ_x, but it is very likely that the effect seen in figure 4 will apply to DNS also. Periods in DNS of the order of $8h$ as in Lee and Kim accommodate only two pairs of vortices, and therefore strongly constrain the period of the vortices which can develop. In particular, efforts which would be very timely to determine the "DNS Answer" for the law of the wall in the region $y^+ \approx 1000$ and the exact value of R_s would definitely be tainted by the arbitrary DNS period unless it reaches values of the order of $20h$, and probably more. This was concluded by Tuskahara et al (2006). Their careful study of DNS periods produced shifts of up to 0.5 units in U^+, which very comparable with ours and is larger than the uncertainty expected of DNS. The dependence of

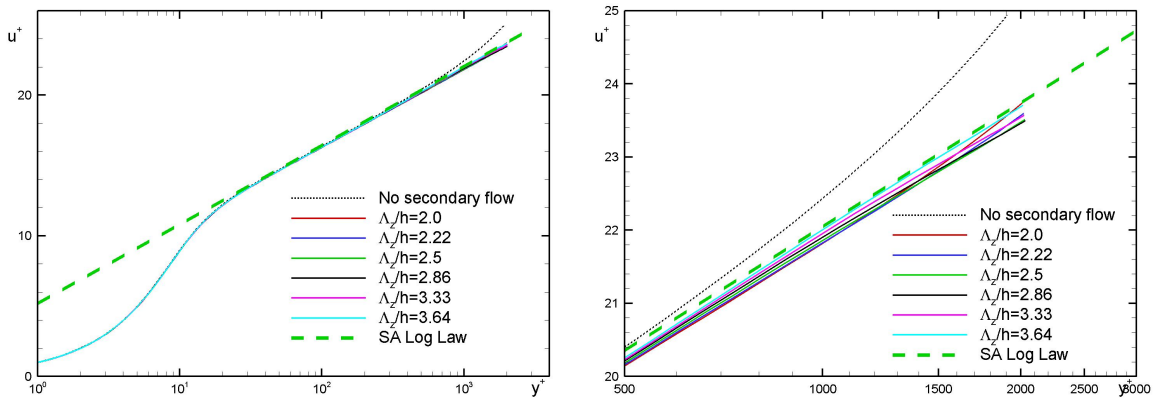

Figure 4. Velocity profiles in wall units.

R_s on Λ_z/h will be displayed in figure 6. We fully recognize that RANS results are not authoritative, but the physical reasoning appears quite convincing.

Figure 5a adds insight into the flow field, with the z dependence of the skin-friction coefficient. It has narrow minima at the convergence lines, lower than the C_f of the 2D solution, between wide maxima which are responsible for the average value being larger than with 2D. The ratio of minimum to maximum goes as low as 0.6; by this measure, the secondary motion is quite strong. Kitoh et al. measured a ratio near 0.75 so that, again, the quantitative agreement is not perfect.

Figure 5b presents the dependence of the mean C_f (here normalized by the C_f calculated without vortices) on period and Reynolds number. It is rather weak, and most likely agrees with a two-layer model of the flow with the law of the wall and a "center law." Within this model, the effect on C_f weakens with higher Reynolds number.

In Figure 6a we display the sensitivity of R_s to spanwise period, at three Reynolds numbers. The effect of the vortices is only weakly dependent on Reynolds number, and peaks for $\Lambda_z/h \approx 3$. This is not very close to the value cited by Kitoh et al., namely about 4. They observed it from the gradual development of an isolated disturbance in z, and therefore it can be considered as "natural." Lee & Kim (1991) also arrived at a value near 4, from DNS (their domain allowed spacings of 4.2 and 2.8, so that the selection of 4.2 appears meaningful). Their R_s was about 2.9. Tsukahara et al. (2009) had somewhat different results: $R_s = 3.14$ and Λ_z/h in the range 4.2–5.

The comparison with experiments, between figures 6a and 6b, is intriguing; the R_s axis was drawn to the same scale in both. We use R_s as a primary measure of the dynamics in the center region; it is the region of interest, because the near-wall behavior follows the usual law of the wall well. Stronger turbulence/eddy viscosity lowers R_s. Classical turbulence theory predicts that R_s is a universal constant, but data collected by Kitoh et al. (2005) range all the way from 2.6 to 5.8. We see no definite Reynolds-number trend, except internally for Kitoh et al.'s own results, but these measurements were intentionally made at very low Reynolds numbers. There is no suggestion that this comes from "low-Reynolds-number effects" and disappears once *Re* is sufficiently large; we consider facility size and other details to be much more likely sources of the discrepancies. DNS results are all low, somewhat above 3, and all these solutions were marked by large vortices. Kitoh's experiment had these same two features. SA RANS results without vortices are near 5, and results with vortices to date fall between 2.4 and 3.4. This leads us to the *conjecture* that experimental flows with high R_s values for some reason failed to develop the vortices, and therefore depend almost entirely on fine- and medium-scale momentum transfer. If so, they would be more similar to boundary layers and Poiseuille flows, and reasonably well predicted by the RANS models which were adjusted for these flows (which do not grow streamwise vortices, except with concave curvature of course).

The comparison with experiment concludes with Figure 7. Recall that C_f minimizes differences, compared with R_s. CFD results with and without vortices fall within the experimental scatter again, so that this figure is not discriminating. We note that the experiments here are now old, and measuring skin friction is challenging.

Secondary Results

Unsteady simulations starting from infinitesimal perturbations of the 2D solution successfully produced exponential decay or growth after a transient, with growth if $1.42 < \Lambda_z/h < 3.36$. The highest growth rate is present with Λ_z/h slightly over 2, which is certainly smaller than the value which gives the strongest effect in the converged nonlinear solutions, namely about 3.1. The upper stability boundary is also at $\Lambda_z/h \approx 3.36$, when nonlinear solutions were found with 3.64. Linear and nonlinear stability are never identical. This represents hysteresis, but one which appears to take place over a narrow range of values for Λ_z/h.

The SARC model, with a correction aimed at rotation and curvature effects (Shur et al. 2000), had very little effect. This is probably because streamline curvature is weak, and the vortices' rotation rate very slow compared with the shear rates. The SST model, with QCR, produced vortices very much like the SA-QCR model, but we had convergence failures for Λ_z/h smaller than about 3 (Menter 1993).

Finally, the BSL WJ Explicit Algebraic Reynolds-Stress Model of Menter et al. (2009) did not sustain vortices in Couette flow. Thus, capturing the difference between $\overline{w'^2}$ and $\overline{v'^2}$ does not in itself lead to the hoped-for behavior. Naturally, this has been established only for one of many EARSM's on offer.

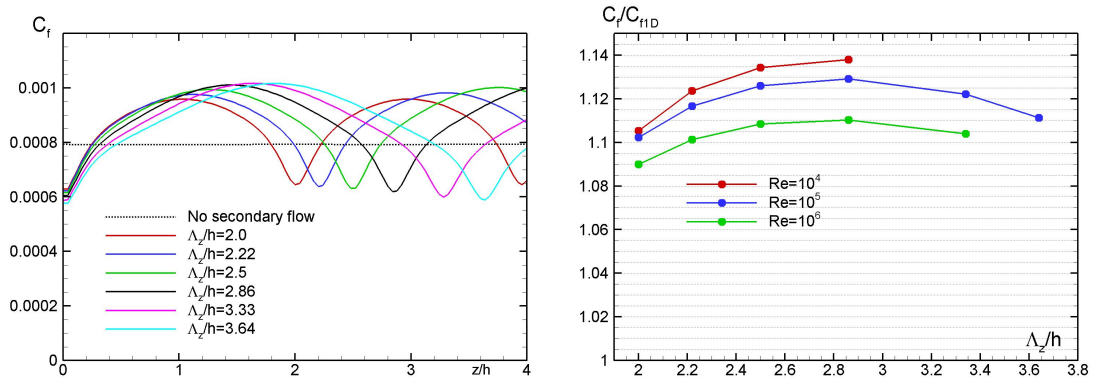

Figure 5. Skin-friction coefficient C_f in the z direction, with and without vortices.

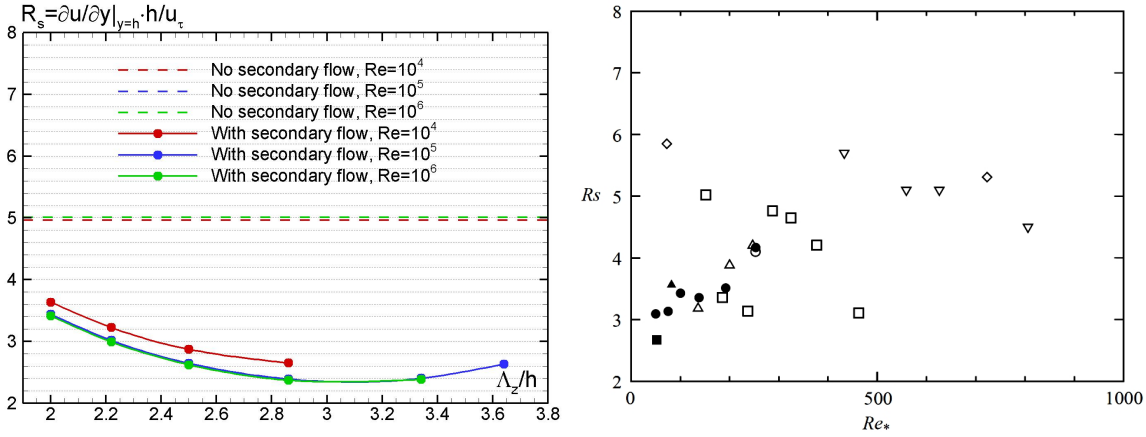

Figure 6. Dependence of R_s on the lateral period and the Reynolds number. Left, CFD with and without vortices; right, experiments (Kitoh et al. 2005).

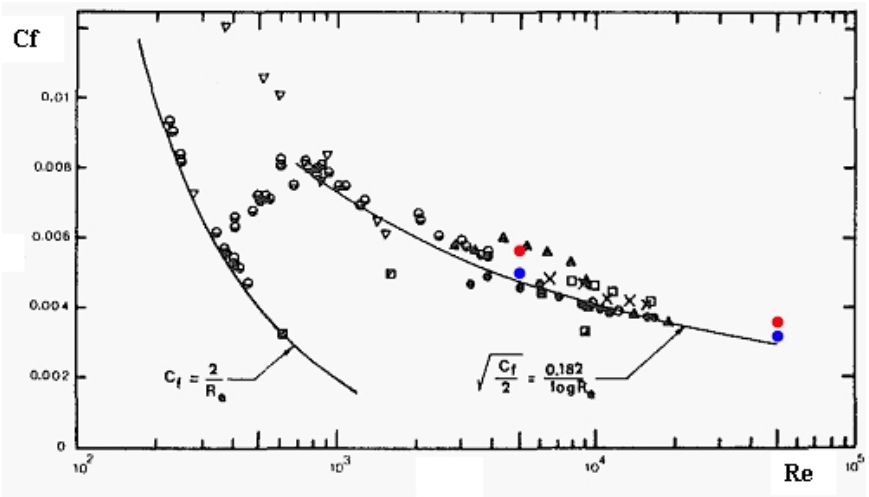

Figure 7. Comparison of C_f with experimental results, collected by El Telbany & Reynolds (1982). Re and C_f are here defined using $U_w/2$ instead of U_w, which introduces factors of 2. Black symbols, experiments; blue, CFD without vortices; red, CFD with vortices.

OUTLOOK

This study exercises a seemingly novel mode of operation for a RANS model by which it tolerates, or in fact generates, flow features with a lateral scale much smaller than the scale of the geometry (which here is infinite) and random locations. This makes these structures very different in nature from corner vortices, which are deterministic, although both respond strongly to QCR. The general effect in Couette flow is to improve the results. Recall that this is without any changes to the model of a Large-Eddy Simulation nature. Therefore, this behavior may appear spontaneously in three-dimensional RANS solutions, and raise the grid resolution needed. It is likely concave curvature will cause the formation of Görtler vortices, but this may

or may not depend on QCR and similar terms as it does for Couette flow. The behavior observed here is reminiscent of the Scale-Adaptive Simulation approach, but we view the similarity as superficial, since SAS is unsteady and aims at simulations with the nature of an LES (Menter et al. 2003).

Future work could include the SST and similar base models, non-linear eddy-viscosity constitutive relations other than QCR, as well as new Algebraic Reynolds Stress and full Reynolds-Stress Transport models. After corner flows, this is the second class of flows to bring out qualitative effects of the QCR. The features needed for a RANS model to generate vortices in Couette flow deserve to be studied, as does the possibility that the wide experimental scatter for R_s is indeed caused by the very sensitive development of the global quasi-steady vortices, and that RANS in an uncertain but nevertheless meaningful way is uncovering this fact.

REFERENCES

El Telbany, M.M.M., Reynolds, A.J. 1982 The Structure of Turbulent Plane Couette Flow. *J. Fluids Eng.* **104**, 367-372.

Kitoh, O., Nakabyashi, K., Nishimura, F. 2005 Experimental study on mean velocity and turbulence characteristics of plane Couette flow: low-Reynolds-number effects and large longitudinal vertical structure. *J. Fluid Mech.* **539**, 199-227.

Kitoh, O., Umeki, M. 2008 Experimental study on large-scale streak structure in the core region of turbulent plane Couette flow. *Phys. Fluids,* **20**, 025107.

Komminahoi, J., Lundbladh, A., Johansson, A. V. 1996 Very large structures in plane turbulent Couette flow. *J. Fluid Mech.* **320**, 259-285.

Lee, M.J., Kim, J. 1991 The structure of turbulence in simulated plane Couette flow. In *Proc. 8th Symp. on Turb. Shear Flows*, 5.3.1.-5.3.6.

Menter, F.R. 1993 Zonal two equation k-ω turbulence models for aerodynamic flows. AIAA Paper 93-2906.

Menter, F.R., Kuntz, M. Bender, R. 2003 A scale-adaptive simulation model for turbulent flow predictions. AIAA Paper 2003-0767.

Menter, F.R., Garbaruk, A.V., Egorov, Y. 2009 Explicit Algebraic Reynolds Stress Models for Anisotropic Wall-Bounded Flows. Proceedings of EUCASS - 3rd European Conference for Aero-Space Sciences.

Robertson, J.M., Johnson, H.F. 1970 Turbulence Structure in Plane Couette Flow. *J. Eng. Mech. Div. Proc. ASCE* **96**, 1171-1182.

Shur, M., Strelets, M., Travin, A., Spalart, P.R. 2000 Turbulence modeling in rotating and curved channels: assessing the Spalart-Shur term. *AIAA J.* **38**, 5, 784-792.

Shur, M., Strelets, M., Travin, A. 2004 High-order implicit multi-block Navier-Stokes code: Ten-year experience of application to RANS/DES/LES/DNS of turbulence. In *Proc. 7th Symp. Overset Composite Grids & Solution Technology*, Huntington Beach, California.

Spalart, P.R., Allmaras, S.R. 1994 A one-equation turbulence model for aerodynamic flows. *Recherche Aérospatiale* **1**, 5-21.

Spalart, P.R. 2000 Strategies for turbulence modelling and simulations. *Int. J. Heat Fluid Flow* **21**, 252-263.

Tsukahara, T., Kawamura, H., Shingai, K. 2006 DNS of turbulent Couette flow with emphasis on the large-scale structure in the core region. *J. Turb.* **7**, No. 19.